

# Discrimination of natural colors in anomalous trichromacy and the effects of EnChroma and Vino filters

DORA N. MARQUES,<sup>\*</sup>  ANDREIA E. GOMES,   
JOÃO M. M. LINHARES,  AND SÉRGIO M. C. NASCIMENTO 

*Physics Center of Minho and Porto Universities (CF-UM-UP), Gualtar Campus, University of Minho, 4710-057 Braga, Portugal*

*\*doranmarques@gmail.com*

**Abstract:** It is still unclear how well anomalous trichromats discriminate natural colors and whether commercial spectral filters improve performance in these conditions. We show that anomalous trichromats have good color discrimination with colors drawn from natural environments. It is only about 14% poorer, on average, than normal trichromats in our sample of thirteen anomalous trichromats. No measurable effect of the filters on discrimination was found, even after 8 hours of continuous use. Computations of cone and post-receptoral signals show only a modest increase in medium-to-long-wavelength difference signals, which may explain the absent effect of the filters.

© 2023 Optica Publishing Group under the terms of the [Optica Open Access Publishing Agreement](#)

## 1. Introduction

Normal color vision in humans is trichromatic, and it is mediated by three types of photoreceptors, the cones, each containing a photopigment with absorption curves peaking in different parts of the visible spectrum. These are the long- (L-), middle- (M-), and short- (S-) wavelength sensitive photopigments [1,2], named according to the spectral location of maximum light absorption.

X-linked red-green color vision deficiency is the most common congenital abnormal visual condition in males: it can affect almost 8% of European Caucasians and 6.5% of Chinese and Japanese [3]. The deficiency can be classified as protan or deutan if it affects the L- or M-photopigment, respectively. It can also be classified by severity as anomalous trichromacy if three photopigments are present (protanomaly when the L-photopigment is absent but a modified form of the M-photopigment is present, and deuteranomaly when the M-photopigment is absent but a modified form of the L-photopigment is present), or as dichromacy if only two photopigments are present [4,5].

Normal trichromatic observers have a spectral separation of about 30 nm between L- and M-cone photopigments [6], whereas the separation in anomalous trichromats is at most 10 nm [7,8]. In protanomaly, the modified M-photopigments are shifted towards longer wavelengths, and, in deuteranomaly, the modified L-photopigments are shifted towards shorter wavelengths [7]. These spectral shifts determine the extent of the anomaly, producing color discrimination with variable impairment, from as good as normal trichromats to almost as poor as dichromats [9–12]. Genotype, photopigment optical density, and peak spectral sensitivity are some of the factors that may account for such variability [12]. There is, however, evidence that anomalous trichromats have post-receptoral mechanisms that partially amplify the smaller difference in medium-to-long-wavelength cone signals [13–16], probably at the cortical level [17].

Anomalous trichromats seem to perform relatively well in everyday life and in several specific visual functions, e.g. color constancy [18,19], and color appearance measured with hue scaling [15] and with color matching of both narrow- and broad-band lights [20]. But measurements of chromatic discrimination are normally carried out in the laboratory with artificial stimuli

that do not represent the ecological physics of the natural environment. These clinical tests, e.g. the Farnsworth-Munsell 100-Hue Test [21,22], the Colour Assessment and Diagnosis test (CAD) [23,24], the Cambridge Colour Test (CCT) [9], and Ishihara color plates test, quantify color confusions without taking into account how frequently the different colors occur in nature. Because natural reflectance spectra are highly constrained [25,26], natural colors have a characteristic chromatic distribution and statistics, lying mainly along a yellow-blue axis of color space [27–30]. Thus, pairs of colors confounded by color deficient individuals may be rare in nature, and therefore have little effect on their average performance. This was indeed found to be true for dichromats, who were only a little worse than normal trichromats in discriminating colors from natural environments [31].

The availability of commercial lenses or filters to improve color vision of the color deficient population has a long history [32–35] and the search for new products continues [36,37]. Yet, so far, there is little scientific consensus on the advantage of using these products [38,39]. Recently, commercial marketing campaigns have focused their attention on specific notch filters, e.g., EnChroma and Vino filters. EnChroma filters are designed to enhance color perception [40]. There are several versions available, for outdoor or indoor use [41]. Vino filters were primarily designed for enhancing the appearance of skin color changes related to blood volume and oxygenation [42], but now these filters are also advertised for color vision deficient individuals [43].

Previous studies found that EnChroma and Vino filters change the overall color appearance but are unable to provide normal discrimination [44–47]. In fact, both may reduce the perceived chromatic diversity by reducing the number of discernible colors [48]. On the other hand, long-term adaptation (two weeks) to these types of filters may produce adaptive post-receptoral changes resulting in an improved discrimination [49]. Although spectral information from natural scenes has been used in previous studies to model color perception with these filters [44,45,48], no empirical measurements of discrimination were carried out.

The purpose of this study was twofold: first, to empirically assess the degree of impairment in chromatic discrimination of anomalous trichromats when viewing colors from natural environments and second, to assess if that discrimination is enhanced with EnChroma and Vino filters. Critically, the assessment was based on the mean performance across the tested scenes rather than on the discrimination in specific chromatic directions or with specific pairs of colors for which performance may be particularly good or bad. Spectral data from hyperspectral imaging of natural scenes were used to produce a real 3D scene simulating naturally colored objects to be discriminated in each trial. Anomalous trichromats were found to have good color discrimination, about 14% poorer than normal trichromats. EnChroma and Vino filters, although enhancing the separation between medium-to-long-wavelength cone signals, did not improve chromatic discrimination, even after 8 hours of continuous use.

## 2. Material and methods

### 2.1. Observers

Thirteen anomalous trichromats were recruited from our laboratory database and by advertising in the social networks of the University of Minho. They comprised 9 deuteranomalous trichromats (7 males, mean age 38 yr, SD 13 yr, and 2 females, mean age 30 yr, SD 7 yr) and 4 protanomalous trichromats (all males, mean age 25 yr, SD 2 yr). One of the deuteranomalous observers was a co-author of this paper and participated only in the first part of the experiment. As a control, 13 observers with normal color vision also participated (5 males, mean age 23 yr, SD 2 yr, and 8 females, mean age 22 yr, SD 2 yr). All control participants were students from the University and were recruited through the students' social networks. The color vision of the observers was tested with Ishihara color plates, Rayleigh Anomaloscope (Oculus Heidelberg Multi Color), and the Colour Assessment and Diagnosis (CAD) Test (version 2.3.1.1, City Occupational Ltd.)

[50]. The classification of the color vision of the observers was based on the mid-point of their Rayleigh matches. Table 1 shows the average anomaly quotient obtained with the anomaloscope and the red-green and yellow-blue thresholds obtained with the CAD test, expressed in Standard Normal Units (SNU) (one SNU relates to the median threshold for a normal population [51,52]). All observers had normal or corrected-to-normal visual acuity. The experiment followed the principles of the Declaration of Helsinki, and informed consent was obtained from all observers.

**Table 1. Anomaly quotients obtained with the anomaloscope and red-green (RG) and yellow-blue (YB) thresholds obtained with the CAD test, expressed in Standard Normal Units (SNU) (one SNU relates to the median threshold for a normal population) [51,52]**

Observers	D1	D2	D3	D4	D5	D6	D7	D8	D9	P1	P2	P3	P4
Anomaly quotient	3.3	3.0	3.5	1.8	5.3	2.4	3.5	3.0	2.8	0.5	0.2	0.2	0.3
RG threshold	2.3	3.5	23.7	20.5	14.4	20.0	2.8	2.3	3.3	19.8	5.3	6.2	22.8
YB threshold	1.7	1.5	1.6	1.1	0.9	1.0	1.4	1.1	1.2	1.0	1.0	1.7	1.4

## 2.2. Filters

Three different filters were tested: Oxy-Iso Color Blindness Clip-on 1.5 mm Lens Blanks from Vino Optics (Vino) assembled in a conventional acetate spectacles frame. Two other filters from EnChroma Color Blind Glasses, the Receptor 64-14-150 BLK 02 (EnChroma R) and the Explorer MTSLV 03 (EnChroma E) were tested in the original frames sold by the company. All identification marks in each frame were concealed to ensure single-blind conditions. The EnChroma filters (EnChroma R and E) were designed for outdoor use and were used here since the experiment simulated natural outdoor scenes. There is only one type of Vino filters for indoor and outdoor use. The Vino filters were obtained in 2019 and the EnChroma filters in 2015. The spectral transmittance of each filter was measured with a Shimadzu UV-3600i Plus UV-VIS-NIR spectrophotometer (Shimadzu Scientific Instruments, Inc.) in the spectral range 400–720 nm with a spectral resolution of 0.1 nm. (Fig. 1). Measurements were carried out with the geometry 0/0 in different positions of the lenses. Variations of transmittance with measuring position across the lenses were negligible.

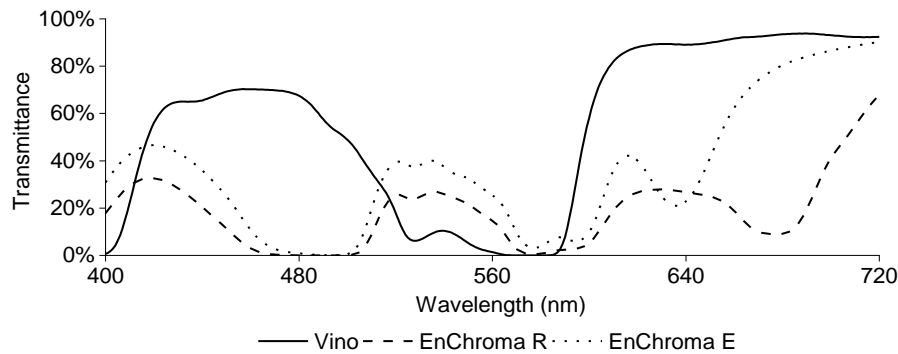


**Fig. 1.** Spectral transmittance of the tested filters. Data obtained with a Shimadzu UV-3600i Plus UV-VIS-NIR spectrophotometer (Shimadzu Scientific Instruments, Inc.).

## 2.3. Experimental setup

The experimental setup (Fig. 2) was adapted from a previous study and is fully described elsewhere [31]. Only the essential features are reported here. The observer was seated at 147 cm

from the scene. A white Styrofoam mask stood at 93 cm from the observer making a visual angle of  $57^\circ \times 79^\circ$ . The test scene was located behind the mask, inside an illumination box painted with Munsell N7 paint (VeriVide Ltd, Leicester, UK). The scene consisted of 3 geometric figures (cylinder, sphere, and parallelepiped) that were set in an acrylate plate slightly tilted forward. The figures were matte white and approximately Lambertian, with a flat reflectance spectrum in the visible region of the spectrum. The visual angle of the scene was  $10^\circ$ . Viewing conditions were monocular to avoid diplopia induced by the setup.

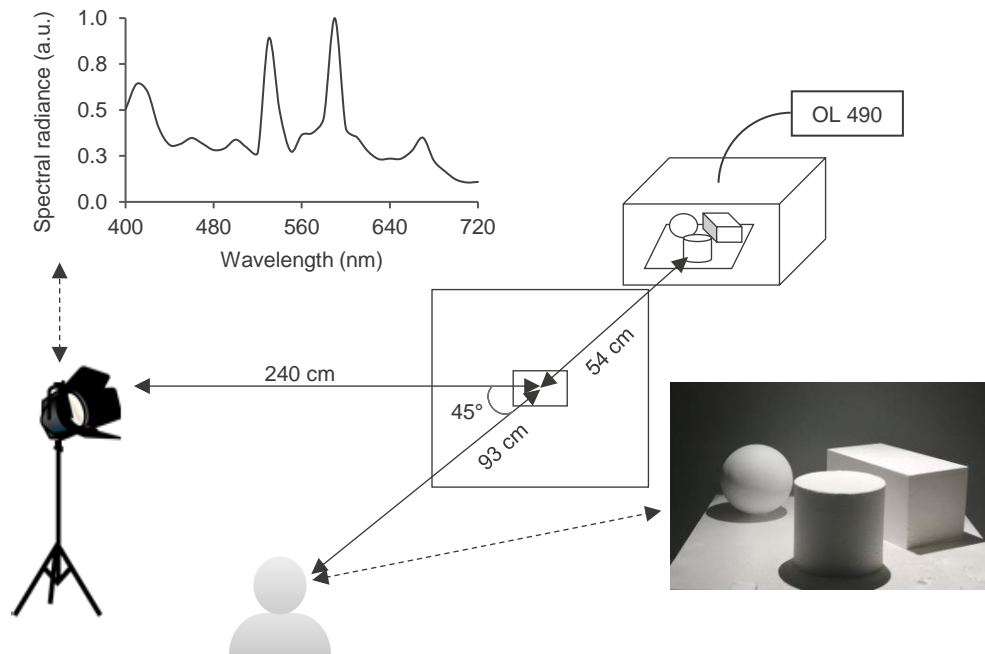


**Fig. 2.** Schematics of the setup for the psychophysical experiment, including the radiance spectrum of the adapting illuminant (discharge lamp OSRAM HQI 150W RX7s) reflected by the Styrofoam mask. The test scene comprising 3 geometric figures (cylinder, sphere, and parallelepiped) was illuminated by a spectrally tunable light source (OL 490 Agile Light Source, Gooch & Housego). The test scene was only visible through an aperture at the center of the Styrofoam mask.

A spectrally tunable light source (OL 490 Agile Light Source, Gooch & Housego) calibrated with a spectral resolution of 20 nm was used to deliver light to the scene through an optical fiber guide coupled with an optical diffuser (10DKIT-C2 25°, Newport). This ensured a level of uniformity of about 90% across the scene [31]. A discharge lamp (OSRAM HQI 150W RX7s) was used as the adapting illuminant of the scene and was positioned at  $45^\circ$  relative to the scene and the observer. The adapting illuminant was uniform across the surface of the mask and had a correlated color temperature (CCT) of 5200 K and a luminance of  $30 \text{ cd/m}^2$ . The spectral profile of the discharge lamp is represented in Fig. 2.

#### 2.4. Stimuli

Stimuli were the geometric figures described in section 2.3. They reflected light to simulate, as closely as possible, naturally colored objects instead of objects illuminated by colored lights. For that effect, the illumination was made diffuse, and surfaces were matte. No specular reflections were present. When viewed through the aperture, the figures seemed to be colored objects with

the color of the light field from the discharge lamp. Crucially, in this setup the illumination is very diffuse, and the reflecting surfaces are matte. This contributes to the sensation of colored objects, even for the non-naïve participant. More importantly, the colors are associated with real objects rather than perceived in isolation or aperture mode.

The spectra from the tunable light source were derived from single pixels of two natural scenes obtained with hyperspectral imaging from existing databases [29,53]. The hyperspectral images represented two different settings: a rural and an urban one, both containing a large volume of the color space of natural colors (Fig. 3). Natural colors and natural scenes are interpreted here as containing elements of our everyday life and may include not only vegetation and natural elements but also man-made objects, like the painted wall (Fig. 3). For comparison, the full gamut of 50 natural images replotted from [29] is also represented in Fig. 3.

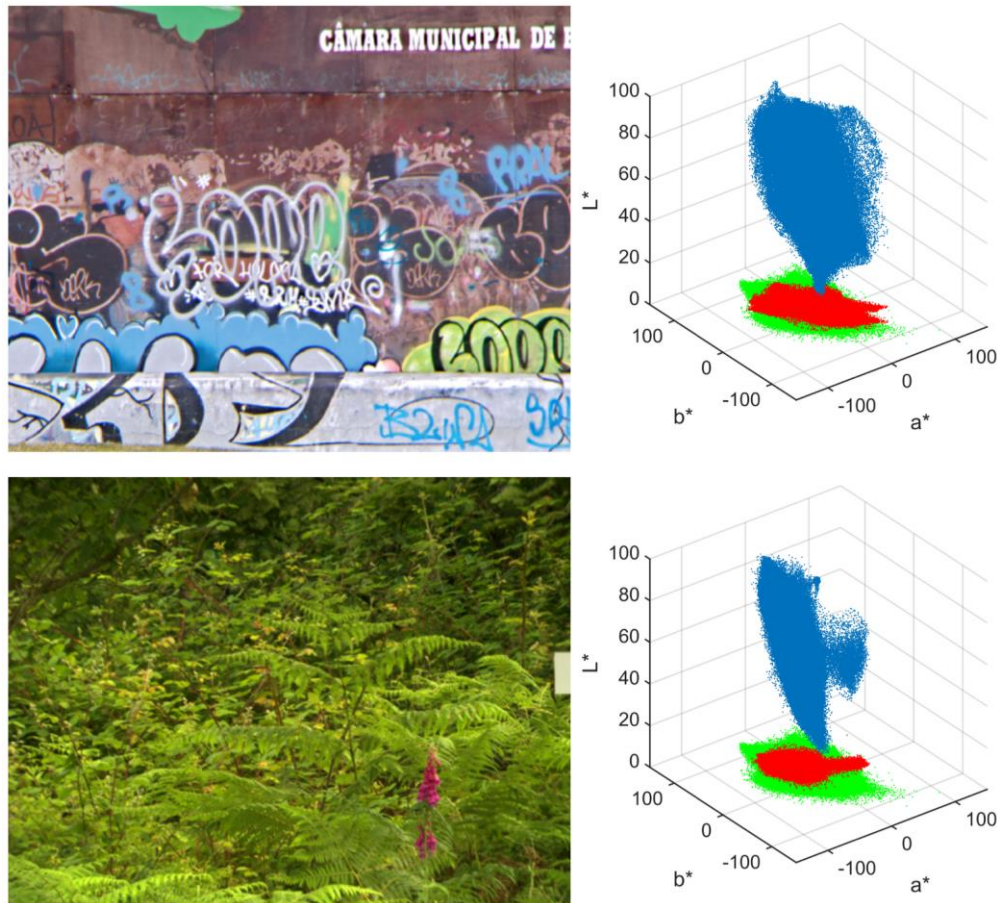


**Fig. 3.** Rendering of the urban (top) and rural (bottom) scenes of the study and their corresponding color volumes. Data were obtained from hyperspectral imaging. The color volumes (blue) are represented in CIELAB color space for the CIE 1964 standard observer and were determined for the adapting illuminant with a CCT of 5200 K. For comparison, the gamut of each scene (red) and of 50 natural images (green) replotted from [29] are projected onto the ( $a^*$ ,  $b^*$ ) plane.



To illustrate the effect of sampling in the conditions of the experiment, Fig. 4 shows independent random samples of 800 spectra from the 2 natural scenes (1300×1024 pixels each). The experiment probed a natural distribution of colors (Fig. 4(b) and 4(c)) and not the natural gamut (Fig. 4(a)).

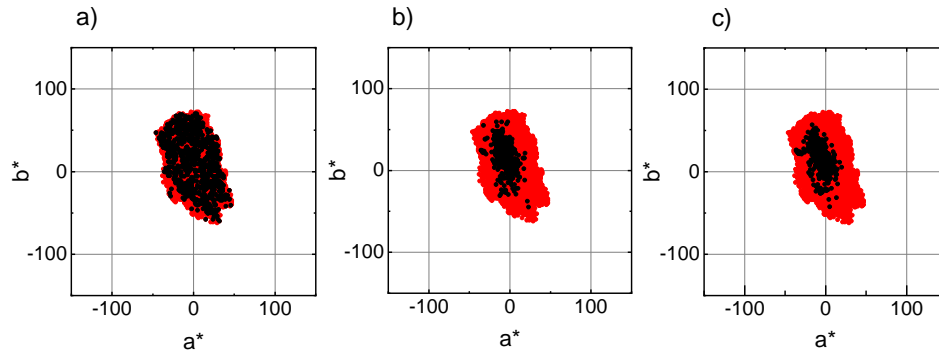


**Fig. 4.** Independent random samples of 800 spectra (black dots) from the two natural scenes tested, with the gamut represented by the red color in all panels: (a) sampling of the gamut (all colors with equal probability); (b) and (c) are two samples of the distribution. Less saturated colors are more likely to be sampled because they occur more often.

## 2.5. Procedure

The experiment was divided into two parts: a first stage without adaptation to the filters and a second stage with an 8-hour adaptation period. In the first stage, there were four conditions tested with spectra derived from each scene in a total of eight sessions: with no filter, with Vino, with EnChroma Receptor, and with EnChroma Explorer. The order of the sessions was randomized, and all were carried out at the same time of the day for each observer. All sessions were set to start between 4 p.m. and 7 p.m., according to the availability of the participants. If the first session was to be conducted at 4 p.m., all the remaining sessions would be conducted at 4 p.m. as well, and so on. Four participants were unable to comply with this schedule, and their sessions in the first stage were all conducted around 10 a.m.

Each session consisted of 220 trials, 20 of which were control trials where the testing spectra were the same to estimate false alarm rates, i.e., the fraction of trials where the observer responds “different” when they are the same [31]. A trial was defined as the test scene being successively illuminated by three lights, separated by a dark inter-stimulus interval of 0.5 s each. The first light was an adapting illuminant that lasted for 1.5 s, which was the same in every trial. The second and third ones were lights extracted from random single pixels sampled with replacement from the test scenes, lasting 0.5 s each [31], and varied in each trial (Fig. 5).

The task of the observers was to decide whether the colors of the objects with the two spectra were the same or different. The answer was given using a control pad (one button for “same” and another one for “different”), in a one-alternative forced choice (1AFC) [54] after each trial. Each observer performed 1,760 trials in this stage.

In a second stage (adaptation), observers used the filters continuously for 8 hours before testing each session, with 8 normal trichromats, 5 deuteranomalous and 4 protanomalous trichromats from the pool of the first stage completing this part of the experiment. There were two conditions with a total of four sessions: with Vino and with EnChroma Receptor filters. Otherwise, the design remained the same as before. The order of the filters and of the sessions was randomized, and all were conducted at the same time of the day of the first stage for each observer. An exception was made for the four participants previously mentioned, who now had their sessions later (5 or 6 p.m.) to comply with the required adaptation period for this stage of the experiment.

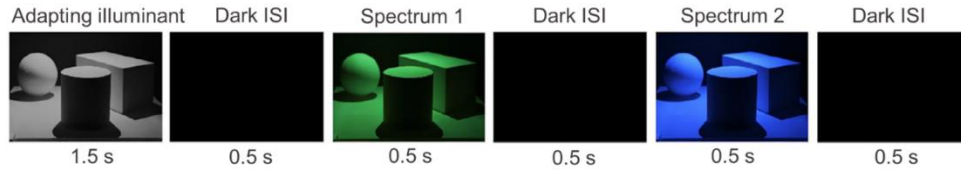


**Fig. 5.** Stimuli sequence in a trial. The adapting illuminant lasted for 1.5 s, followed by spectrum 1 and spectrum 2, each lasting 0.5 s. Between each stimulus, there was a dark inter-stimulus (ISI) interval also of 0.5 s. Spectra 1 and 2 were selected randomly from individual pixels of the scenes tested. The task of the observer was to decide if the colors of the objects illuminated with the two spectra were the same or different.

## 2.6. Computation of cone and post-receptoral signals

To estimate how the filters affect post-receptoral signals, we computed medium-to-long-wavelength difference signals for two independent random samples of 5000 radiance spectra from the two scenes tested. The spectral radiance  $R(x, y; \lambda)$  from each sample, located at each point  $x, y$  in the image at wavelength  $\lambda$ , was obtained by multiplying the spectral reflectance function  $\gamma(x, y; \lambda)$  at each  $x, y$  location obtained from hyperspectral imaging by the spectrum  $I(\lambda)$  of the adapting illuminant, as represented in Fig. 2:

$$R(x, y, \lambda) = I(\lambda)\gamma(x, y; \lambda). \quad (1)$$

For each cone class,  $k$  cone signals  $q_k(x, y)$  were obtained by integration using the corresponding cone spectral sensitivities  $s_k(\lambda)$

$$q_k = \int_{400 \text{ nm}}^{720 \text{ nm}} R(x, y, \lambda) s_k(\lambda) d\lambda. \quad (2)$$

To simulate normal observer responses, we used the Stockman and Sharpe cone spectral sensitivities [6]. To simulate a range of deuteranomalous observers, we shifted the L photopigment spectra by 2, 4, 6, 8 and 10 nm along a normalized wavenumber scale. To simulate a range of protanomalous, we similarly shifted the M photopigment spectra by 2, 4 and 6 nm [8]. Self-screening, and filtering by the macular pigment and the lens were taken into account using the methodology of Stockman and Sharpe [55], and the optical density data from Stockman and colleagues [56]. This procedure produces a plausible range of spectral sensitivities because these are relatively invariant under these transformations [57,58].

Cones were then assumed to be adapted to the illuminant  $I(\lambda)$  by applying a von Kries scaling [59] by the cone signals from the illuminant  $q_k^I$ . This scaling is often used to model adaptation at the photoreceptor level [28,60] but does not incorporate any post-receptoral adaptation. Thus, the scaled cone signals were

$$q'_k = \frac{q_k}{q_k^I}. \quad (3)$$

For the conditions with filters,  $I(\lambda)$  was replaced by  $I(\lambda)f(\lambda)$ , where  $f(\lambda)$  is the spectral transmittance of each filter. Difference signals were computed with and without filters.

## 3. Results

### 3.1. Experiment

Figure 6 summarizes the discrimination by normal and anomalous trichromatic observers in the first stage of the experiment, without adaptation. Two main performance parameters are shown: the discrimination index  $d'$  and the computed discrimination rate assuming that observers all have

the same criterion. The index  $d'$  [61] is a measure of discrimination that is relatively unaffected by the criterion of each observer or observer bias towards responding “same” or “different”. It corresponds to the separation, expressed in units of standard deviation, between the means of the two distributions underlying “same” and “different” internal representations. These two distributions summarize responses to the same stimuli and to different stimuli. Here,  $d'$  was computed assuming a 1AFC, with a differencing model of a same-different task [54,62]. Extreme false alarm rates of zero were replaced by  $0.5/n$  where  $n$  is the number of control (noise) trials [63]. Then,  $d'$  values were inverted to express discrimination performance in a more familiar way, i.e. the pairs of spectra discriminated if all observers had the same criterion.

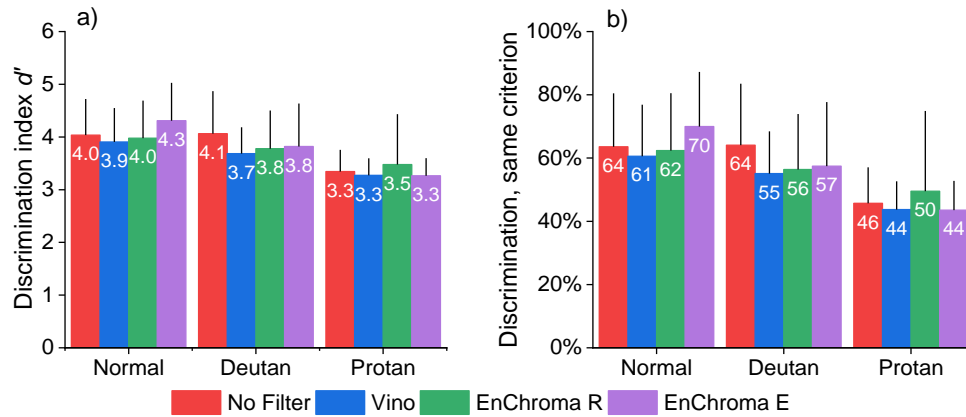


**Fig. 6.** Discrimination without adaptation to the filters (first stage of the experiment). Error bars represent standard deviations across observers. (a) Mean discrimination index  $d'$  computed for a 1AFC, same-different task by the differencing model [54]. (b) Mean fraction of pairs of discriminable colors derived from  $d'$ , assuming that all observers have the same criterion. Data based on 1,760 trials for each observer (13 normal, 9 deuteranomalous and 4 protanomalous trichromats).

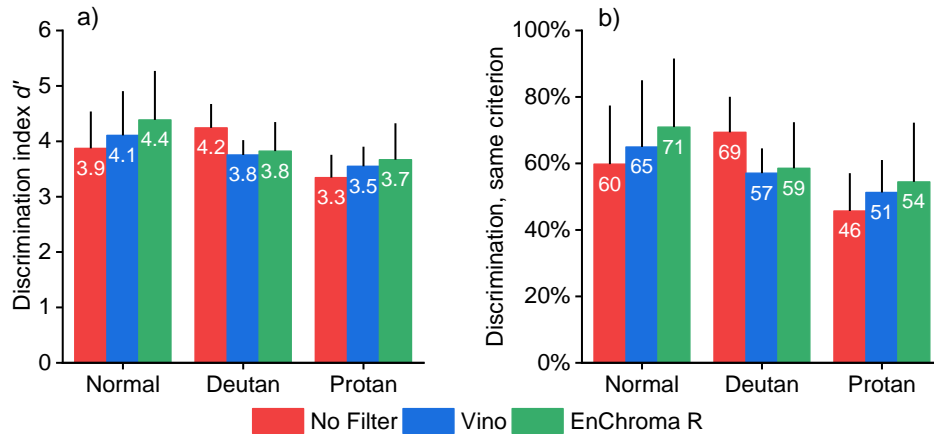
Average false alarm rates for the rural scene were 12% and 15% for normal and anomalous observers, respectively. For the urban scene, they were 10% and 11% for normal and anomalous observers, respectively. The discrimination computed assuming the same criterion was about 64% for normal trichromats, and 64% and 46% for deuteranomalous and protanomalous trichromats, respectively. Thus, only protanomalous trichromats show impairment in discrimination. Repeated-measures ANOVA carried out on the discrimination rates with the same criterion showed no significant effect of the filters for normal trichromats ( $F_{3,36} = 2.58, p = 0.07$ ), for deuteranomalous trichromats ( $F_{3,24} = 1.43, p = 0.26$ ), and for protanomalous trichromats ( $F_{3,9} = 0.56, p = 0.60$ ).

Figure 7 represents data in the same format as Fig. 6 for seventeen observers, 8 normal, 5 deuteranomalous and 4 protanomalous trichromats (all naïve), without filters (data from the first stage) and with filters after 8 hours of use (second stage). Repeated-measures ANOVA carried out on discrimination rates assuming the same criterion showed no significant effect of filters for normal trichromats ( $F_{2,14} = 3.01, p = 0.08$ ) or for anomalous trichromats ( $F_{2,16} = 2.06, p = 0.16$ ).

### 3.2. Post-receptoral signals

Figure 8 shows the standard deviations of the distributions of post-receptoral medium-to-long-wavelength difference signals for each spectral separation, with and without filters. For simulated deuteranomalous observers, the filters induced an effective separation between the difference signals shown by larger standard deviations. For protanomalous observers, the effect occurs only





**Fig. 7.** Discrimination without filters (from the first experimental stage) and after an 8-hour adaptation period with filters Vino and EnChroma Receptor (second experimental stage) for the 17 observers who completed the study (8 normal, 5 deuteranomalous and 4 protanomalous trichromats). Error bars represent standard deviations across observers. (a) Mean discrimination index  $d'$  computed for a 1AFC, same-different task by the differencing model [54]. (b) Mean fraction of pairs of discriminable colors derived from  $d'$ , assuming that all observers have the same criterion. Data included 1,320 trials for each observer (440 without filters from the first stage, and 880 with both filters in the second stage).

for the Vino filter. The perceptual consequence of this separation could be an increase in the perceived saturation of the corresponding colors.

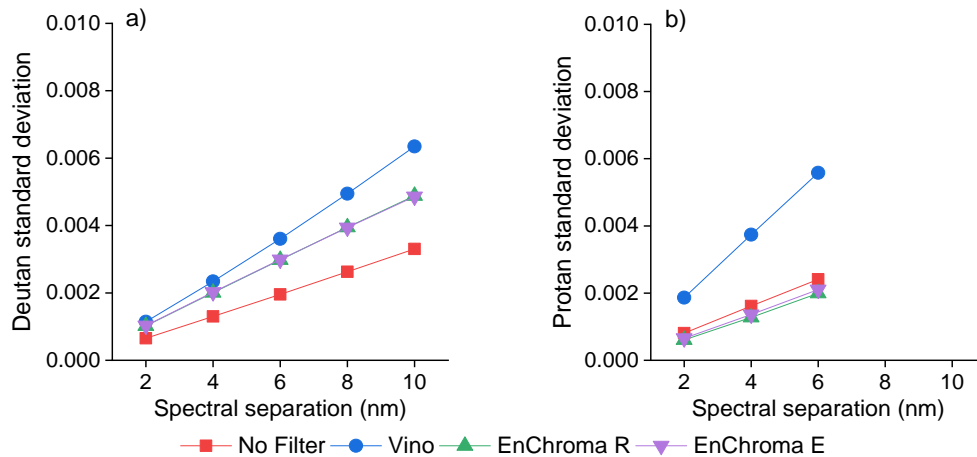


**Fig. 8.** Standard deviations of the distributions of post-receptoral medium-to-long-wavelength difference signals for each spectral separation (in nm) with and without filters for simulated deuteranomalous (a) and protanomalous (b) observers.

What was tested here, however, was the discrimination between pairs of surfaces and this is driven by some form of contrast between signals. Contrast has been used in many conditions, e.g., for quantifying conspicuity [64] and color and luminance edges in natural scenes [65,66].

There is not, however, a standard way to compute contrast. Inspired by measures of contrast for colored edges in natural scenes [66], we computed a contrast measure as follows. Let  $S_1$  and  $S_2$  be the medium-to-long-wavelength difference signals from two sample surfaces. The contrast  $C$  was computed as

$$C = \frac{|S_1 - S_2|}{\max(|S_1|, |S_2|)}. \quad (4)$$

This formulation of contrast measures a relative variation avoiding artifacts due to small values in the denominator. Figure 9 shows the mean contrast of post-receptoral medium-to-long-wavelength difference signals for each spectral separation, with and without filters. The increase in contrast with filters is at most a few percent, which may explain the neutral effects of the filters on discrimination performance.

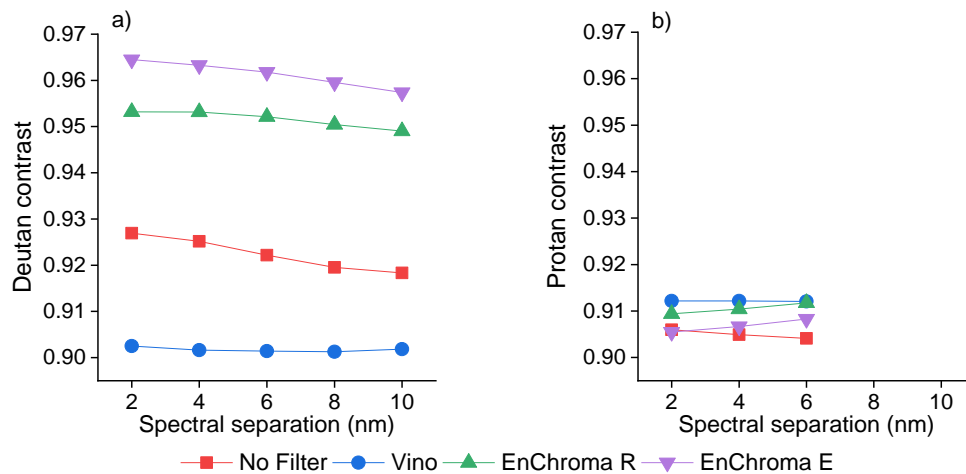


**Fig. 9.** Mean contrast of post-receptoral medium-to-long-wavelength difference signals for each spectral separation (in nm) with and without filters for simulated deuteranomalous (a) and protanomalous (b) observers.

#### 4. Conclusions

The first conclusion is that anomalous trichromats seem to show little impairment in discriminating randomly selected colors from natural scenes. This is consistent with data obtained with a similar experimental paradigm for dichromats [31]. Due to ecological physics [25,67], the colors of natural scenes are mainly distributed along the yellow-blue axis [28,68,69]. This might help the discrimination of certain pairs of colors by both dichromats and anomalous trichromats. Estimates based on optimal color volumes suggest a much larger impairment [70] but those computations assume that all object colors occur with equal probability, which is not the case in nature. It should be noted that stimuli in the experiments were not constrained; thus, discrimination can rely on chromatic channels as well as the achromatic one.

The second conclusion is that neither EnChroma nor Vino filters improve discrimination for the sample of anomalous observers tested with the current paradigm. This is consistent with previous studies that showed no improvement in several standard color vision tests [44–46,71]. Even after an 8-hour adaptation period, the performance of the anomalous observers did not improve. Longer adaptation periods may, however, produce different results [49].

Two important comments should be added. What was assessed in this study was the average discrimination in the tested scenes, and the filters may improve discrimination for some specific

pairs of colors or specific color directions. Also, apart from trying to improve discrimination, there may be other reasons for anomalous trichromats to use these filters. For example, they may prefer the modified color appearance that the filters give to objects.

More generally, the experimental methodology used here has several advantages in relation to laboratory tests reported previously. It allows natural colors to be tested without the gamut constraints of RGB monitors, does not require any assumptions about the cone spectral sensitivities of anomalous trichromats, and eliminates contextual cues which may influence color deficient observers [72]. Strictly, this notion of naturalness applies only to the spectral reflectance data as the laboratory setup does not reproduce the natural visual environment.

The computations of post-receptoral medium-to-long-wavelength difference signals show that the filters may indeed have an enhancing effect on their amplitude but their contrast changes only a few percent, a result which is broadly consistent with limited theoretical gains derived from information theory [73].

In summary, the data presented here do not support the effectiveness of EnChroma or Vino filters for improving discrimination by anomalous trichromats of randomly selected colors from natural scenes, at least during or after one-day's adaptation.

**Funding.** Fundação para a Ciência e a Tecnologia (UIDB/FIS/04650/2020); Fundação para a Ciência e a Tecnologia/Fundo Social Europeu (2020.05785.BD)

**Acknowledgments.** We are grateful to the observers for their patience and dedication.

**Disclosures.** The authors declare no conflicts of interest related to this paper.

**Data availability.** Data underlying the results presented in this paper are not publicly available at this time but may be obtained from the authors upon reasonably justified request.

## References

1. S. L. Merbs and J. Nathans, "Absorption spectra of human cone pigments," *Nature* **356**(6368), 433–435 (1992).
2. S. G. Solomon and P. Lennie, "The machinery of colour vision," *Nat. Rev. Neurosci.* **8**(4), 276–286 (2007).
3. J. Birch, "Worldwide prevalence of red-green color deficiency," *J. Opt. Soc. Am. A* **29**(3), 313–320 (2012).
4. J. D. Mollon, J. Pokorny, and K. Knoblauch, *Normal and Defective Colour Vision* (Oxford University Press, 2003).
5. P. DeMarco, J. Pokorny, and V. C. Smith, "Full-spectrum cone sensitivity functions for X-chromosome-linked anomalous trichromats," *J. Opt. Soc. Am. A* **9**(9), 1465–1476 (1992).
6. A. Stockman and L. T. Sharpe, "The spectral sensitivities of the middle- and long-wavelength-sensitive cones derived from measurements in observers of known genotype," *Vision Res.* **40**(13), 1711–1737 (2000).
7. J. Neitz and M. Neitz, "The genetics of normal and defective color vision," *Vision Res.* **51**(7), 633–651 (2011).
8. C. Davidoff, M. Neitz, and J. Neitz, "Genetic testing as a new standard for clinical diagnosis of color vision deficiencies," *Trans. Vis. Sci. Tech.* **5**(5), 2–16 (2016).
9. B. C. Regan, J. P. Reffin, and J. D. Mollon, "Luminance noise and the rapid determination of discrimination ellipses in colour deficiency," *Vision Res.* **34**(10), 1279–1299 (1994).
10. J. M. M. Linhares, C. A. R. Joao, V. M. N. de Almeida, J. L. A. Santos, L. Alvaro, and S. M. C. Nascimento, "Assessing the effects of dynamic luminance contrast noise masking on a color discrimination task," *J. Opt. Soc. Am. A* **33**(3), A178–A183 (2016).
11. J. Barbur, M. Rodriguez-Carmona, S. Evans, and N. Milburn, *Minimum Color Vision Requirements for Professional Flight Crew, Part III: Recommendations for New Color Vision Standards* (Applied Vision Research Center, City Univ London, 2009).
12. J. Bosten, "The known unknowns of anomalous trichromacy," *Current Opinion in Behavioral Sciences* **30**, 228–237 (2019).
13. A. E. Boehm, D. I. A. MacLeod, and J. M. Bosten, "Compensation for red-green contrast loss in anomalous trichromats," *Journal of Vision* **14**(13), 19 (2014).
14. K. Knoblauch, B. Marsh-Armstrong, and J. S. Werner, "Suprathreshold contrast response in normal and anomalous trichromats," *J. Opt. Soc. Am. A* **37**(4), A133–A144 (2020).
15. K. J. Emery, M. Kuppaswamy Parthasarathy, D. S. Joyce, and M. A. Webster, "Color perception and compensation in color deficiencies assessed with hue scaling," *Vision Res.* **183**, 1–15 (2021).
16. J. E. Vanston, K. E. M. Tregillus, M. A. Webster, and M. A. Crognale, "Task-dependent contrast gain in anomalous trichromats," *Vision Res.* **184**, 14–22 (2021).
17. K. E. M. Tregillus, Z. J. Isherwood, J. E. Vanston, S. A. Engel, D. I. A. MacLeod, I. Kuriki, and M. A. Webster, "Color compensation in anomalous trichromats assessed with fMRI," *Curr. Biol.* **31**(5), 936–942.e4 (2021).
18. R. C. Baraas, D. H. Foster, K. Amano, and S. M. C. Nascimento, "Color constancy of red-green dichromats and anomalous trichromats," *Investig. Ophthalmol. Vis. Sci.* **51**(4), 2286–2293 (2010).

19. R. C. Baraas, D. H. Foster, K. Amano, and S. M. C. Nascimento, "Anomalous trichromats' judgments of surface color in natural scenes under different daylights," *Vis Neurosci* **23**(3-4), 629–635 (2006).
20. D. T. Lindsey, A. M. Brown, and L. N. Hutchinson, "Appearance of special colors in deuteranomalous trichromacy," *Vision Res.* **185**, 77–87 (2021).
21. J. Moreland, V. Cheung, and S. Westland, "Evaluation of a model to predict anomalous-observer performance with the 100-hue test," *J. Opt. Soc. Am. A* **31**(4), A125–A130 (2014).
22. N. V. O. Bento-Torres, A. R. Rodrigues, M. I. T. Côrtes, D. M. D. O. Bonci, D. F. Ventura, and L. C. D. L. Silveira, "Psychophysical evaluation of congenital colour vision deficiency: Discrimination between protans and deutans using Mollon-Reffin's ellipses and the Farnsworth-Munsell 100-hue test," *PLoS One* **11**(4), e0152214 (2016).
23. J. L. Barbur and M. Rodriguez-Carmona, "Colour vision requirements in visually demanding occupations," *Br. Med. Bull.* **122**(1), 51–77 (2017).
24. M. Marechal, M. Delbarre, J. Tesson, C. Lacambre, H. Lefebvre, and F. Froussart-Maille, "Color vision tests in pilots' medical assessments," *Aerospace Medicine and Human Performance* **89**(8), 737–743 (2018).
25. J. J. Koenderink, "The prior statistics of object colors," *J. Opt. Soc. Am. A* **27**(2), 206–217 (2010).
26. S. M. C. Nascimento, D. H. Foster, and K. Amano, "Psychophysical estimates of the number of spectral-reflectance basis functions needed to reproduce natural scenes," *J. Opt. Soc. Am. A* **22**(6), 1017 (2005).
27. S. M. C. Nascimento, F. P. Ferreira, and D. H. Foster, "Statistics of spatial cone-excitation ratios in natural scenes," *J. Opt. Soc. Am. A* **19**(8), 1484–1490 (2002).
28. M. A. Webster and J. D. Mollon, "Adaptation and the color statistics of natural images," *Vision Res.* **37**(23), 3283–3298 (1997).
29. J. M. M. Linhares, P. D. Pinto, and S. M. C. Nascimento, "The number of discernible colors in natural scenes," *J. Opt. Soc. Am. A* **25**(12), 2918–2924 (2008).
30. G. J. Burton and I. R. Moorhead, "Color and spatial structure in natural scenes," *Appl. Opt.* **26**(1), 157–170 (1987).
31. R. C. Pastilha, J. M. M. Linhares, A. E. Gomes, J. L. A. Santos, V. M. N. de Almeida, and S. M. C. Nascimento, "The colors of natural scenes benefit dichromats," *Vision Res.* **158**, 40–48 (2019).
32. J. C. Maxwell, "XVIII. – Experiments on colour, as perceived by the eye, with remarks on colour-blindness," *Trans. - R. Soc. Edinburgh* **21**(2), 275–298 (1857).
33. I. M. Siegel, "The X-Chrom Lens. On Seeing Red," *Surv. Ophthalmol.* **25**(5), 312–324 (1981).
34. H. A. Swarbrick, P. Nguyen, T. Nguyen, and P. Pham, "The ChromaGen contact lens system: Colour vision test results and subjective responses," *Ophthalmic Physiologic Optic* **21**(3), 182–196 (2001).
35. O. M. Oriowo and A. Z. Alotaibi, "Chromagen lenses and abnormal colour perception," *African Vis. Eye Heal.* **70**(2), 69–74 (2011).
36. A. R. Badawy, M. U. Hassan, M. Elsharif, Z. Ahmed, A. K. Yetisen, and H. Butt, "Contact lenses for color blindness," *Adv. Healthcare Mater.* **7**(12), 1800152 (2018).
37. S. Karepov and T. Ellenbogen, "Metasurface-based contact lenses for color vision deficiency," *Opt. Lett.* **45**(6), 1379–1382 (2020).
38. R. Huertas, M. A. Martínez-Domingo, E. M. Valero, L. Gomez-Robledo, and J. Hernández-Andrés, "Metasurface-based contact lenses for color vision deficiency: comment," *Opt. Lett.* **45**(18), 5117–5118 (2020).
39. J. D. Moreland, S. Westland, V. Cheung, and S. J. Dain, "Quantitative assessment of commercial filter "aids" for red-green colour defectives," *Ophthalmic Physiol. Opt.* **30**(5), 685–692 (2010).
40. A. W. Schmeder and D. M. McPherson, "Multi-band color vision filters and method by lp-optimization," U.S. patent application US 2021/0141132 A1 (2021).
41. EnChroma, "EnChroma® Color Blind Glasses | Cutting-Edge Lens Technology," <https://enchroma.com/>.
42. T. P. Barber and M. Changizi, "Apparatus and method for orthogonalizing signals detecting blood oxygenation and blood volume," U.S. patent US 9,192,304 B2 (2015).
43. VINO, "VINO Optics Vein Finder Eyewear," <https://www.vino.vi/>.
44. L. Gómez-Robledo, E. M. Valero, R. Huertas, M. A. Martínez-Domingo, and J. Hernández-Andrés, "Do EnChroma glasses improve color vision for colorblind subjects?" *Opt. Express* **26**(22), 28693–28703 (2018).
45. M. A. Martínez-Domingo, L. Gómez-Robledo, E. M. Valero, R. Huertas, J. Hernández-Andrés, S. Ezpeleta, and E. Hita, "Assessment of VINO filters for correcting red-green color vision deficiency," *Opt. Express* **27**(13), 17954–17967 (2019).
46. R. Mastey, E. J. Patterson, P. Summerfelt, J. Luther, J. Neitz, M. Neitz, and J. Carroll, "Effect of "color-correcting glasses" on chromatic discrimination in subjects with congenital color vision deficiency," *Invest Ophthalmol Vis Sci* **57**, 192 (2016).
47. E. J. Patterson, "Glasses for the colorblind: their effect on chromatic discrimination in subjects with congenital red-green color vision deficiency," in *24th International Colour Vision Society Symposium, Erlangen, Germany* (2017), p. 23.
48. M. A. Martínez-Domingo, E. M. Valero, L. Gómez-Robledo, R. Huertas, and J. Hernández-Andrés, "Spectral filter selection for increasing chromatic diversity in CVD subjects," *Sensors* **20**(7), 2023 (2020).
49. J. S. Werner, B. Marsh-Armstrong, and K. Knoblauch, "Adaptive changes in color vision from long-term filter usage in anomalous but not normal trichromacy," *Curr. Biol.* **30**(15), 3011–3015.e4 (2020).
50. B. J. Jennings and J. L. Barbur, "Colour detection thresholds as a function of chromatic adaptation and light level," *Ophthalmic Physiol. Opt.* **30**(5), 560–567 (2010).

51. J. L. Barbur, M. Rodríguez-Carmona, and A. Harlow, "Establishing the statistical limits of "normal" chromatic sensitivity," in *CIE Expert Symposium, CIE Proceedings 75 Years of the Standard Colorimetric Observer* (2006).
52. M. Rodríguez-Carmona, "Variability of chromatic sensitivity: fundamental studies and clinical applications," (Doctoral thesis, City Univ., London), (2006).
53. D. H. Foster, K. Amano, S. M. C. Nascimento, and M. J. Foster, "Frequency of metamerism in natural scenes," *J. Opt. Soc. Am. A* **23**(10), 2359–2372 (2006).
54. F. A. A. Kingdom and N. Prins, *Psychophysics: A Practical Introduction*, 2nd ed. (Academic Press, 2016).
55. A. Stockman and L. T. Sharpe, "Cone spectral sensitivities and color matching," in *Color Vision: From Genes to Perception* (1999), pp. 53–88.
56. A. Stockman, L. T. Sharpe, and C. Fach, "The spectral sensitivity of the human short-wavelength sensitive cones derived from thresholds and color matches," *Vision Res.* **39**(17), 2901–2927 (1999).
57. T. D. Lamb, "Photoreceptor spectral sensitivities: Common shape in the long-wavelength region," *Vision Res.* **35**(22), 3083–3091 (1995).
58. D. H. Foster, "Chromatic Function of the Cones," in *Reference Module in Neuroscience and Biobehavioral Psychology* (Elsevier, 2017), pp. 266–274.
59. J. von Kries, "Chromatic adaptation," in *Sources of Color Science*, D. L. MacAdam, ed. (MIT Press, 1970), pp. 109–119.
60. D. H. Foster, S. M. C. Nascimento, and K. Amano, "Information limits on identification of natural surfaces by apparent colour," *Perception* **34**(8), 1003–1008 (2005).
61. J. A. Swets, W. P. Tanner, and T. G. Birdsall, "Decision processes in perception," *Psychological Review* **68**(5), 301–340 (1961).
62. N. A. Macmillan and C. D. Creelman, *Detection Theory: A User's Guide*, 2nd ed. (Lawrence Erlbaum Associates, 2005).
63. N. A. Macmillan and H. L. Kaplan, "Detection theory analysis of group data. Estimating sensitivity from average hit and false-alarm rates," *Psychological Bulletin* **98**(1), 185–199 (1985).
64. L. M. Arenas, J. Troscianko, and M. Stevens, "Color contrast and stability as key elements for effective warning signals," *Vis Neurosci* **2**, 25 (2014).
65. T. Hansen and K. R. Gegenfurtner, "Independence of color and luminance edges in natural scenes," *Vis. Neurosci.* **26**(1), 35–49 (2009).
66. J. L. Nieves, S. M. C. Nascimento, and J. Romero, "Contrast edge colors under different natural illuminations," *J. Opt. Soc. Am. A* **29**(2), A240–A246 (2012).
67. J. Koenderink and A. van Doorn, "Colors of the sublunar," *i-Perception* **8**, 204166951773348 (2017).
68. M. A. Webster, Y. Mizokami, and S. M. Webster, "Seasonal variations in the color statistics of natural images," *Network: Computation in Neural Systems* **18**(3), 213–233 (2007).
69. C. Montagner, J. M. M. Linhares, M. Vilarigues, and S. M. C. Nascimento, "Statistics of colors in paintings and natural scenes," *J. Opt. Soc. Am. A* **33**(3), A170–177 (2016).
70. E. Perales, F. M. Martínez-Verdú, J. M. M. Linhares, and S. M. C. Nascimento, "Number of discernible colors for color-deficient observers estimated from the MacAdam limits," *J. Opt. Soc. Am. A* **27**(10), 2106–2114 (2010).
71. N. Almutairi, J. Kundart, N. Muthuramalingam, J. Hayes, K. Citek, and S. Aljohani, "Assessment of EnChroma filter for correcting color vision deficiency," (Master's thesis, Pacific Univ.), (2017).
72. A. Almustanyir and J. K. Hovis, "Color vision defectives' experience: When white is green," *Color Res. Appl.* **45**(4), 586–590 (2020).
73. S. M. C. Nascimento and D. H. Foster, "Information gains from commercial spectral filters in anomalous trichromacy," *Opt. Express* **30**, 16883–16895 (2022).